On the Relationship between Inhibition and Receptor Occupancy by Nondepolarizing Neuromuscular Blocking Drugs

Hikaru Hoshino (hoshino@eng.u-hyogo.ac.jp)
University of Hyogo https://orcid.org/0000-0003-2487-8320
Eiko Furutani
University of Hyogo

Research

Keywords: Anesthesia, Neuromuscular blockade, Receptor binding models, Nonlinear relationship

Posted Date: April 1st, 2021

DOI: https://doi.org/10.21203/rs.3.rs-376415/v1

Version of Record: A version of this preprint was published at Theoretical Biology and Medical Modelling on August 21st, 2021. See the published version at https://doi.org/10.1186/s12976-021-00147-w.

RESEARCH

On the Relationship between Inhibition and Receptor Occupancy by Nondepolarizing Neuromuscular Blocking Drugs

Hikaru Hoshino[1*] and Eiko Furutani[1,2]

*Correspondence: hoshino@eng.u-hyogo.ac.jp
[1]Department of Electrical Materials and Engineering, University of Hyogo, Hyogo, Japan
Full list of author information is available at the end of the article

Abstract

Background: Nondepolarizing neuromuscular blocking drugs (NDNBs) are clinically used to produce muscle relaxation during general anesthesia. To better understand clinical properties of NDNBs, comparative *in vitro* pharmacologic studies have been performed. In these studies, a receptor binding model, which relies on the assumption that the inhibition, i.e., the effect of an NDNB, is proportional to the receptor occupancy by the drug, has been effectively used to describe obtained experimental data. However, it has not been studied in literature under which conditions the above assumption can be justified nor the assumption still holds *in vivo*. The purpose of this study is to explore the *in vivo* relationship between the inhibition and the receptor occupancy by an NDNB and to draw implications on how *in vitro* experimental results can be used to discuss the *in vivo* properties of NDNBs.

Methods: An ordinary differential equation model is employed to simulate physiologic processes of the activation of receptors by acetylcholine (ACh) as well as inhibition by an NDNB. With this model, the degree of inhibition is quantified by the fractional amount of receptors that are not activated by ACh due to the presence of an NDNB. The results are visualized by plotting the fractional amounts of the activated receptors as a function of the receptor occupancy.

Results: Numerical investigations reflecting *in vivo* conditions show that the degree of inhibition is not proportional to the receptor occupancy, i.e., there is a nonlinear relationship between the inhibition and the receptor occupancy. However, under a setting of high concentration of ACh reflecting a typical situation of *in vitro* experiments, the relationship between the inhibition and the receptor occupancy becomes linear, suggesting the validity of the receptor binding model. Also, it is found that the extent of nonlinearity depends on the selectivity of NDNBs for the two binding sites of the receptors.

Conclusions: While the receptor binding model may be effective for estimating affinity of an NDNB through *in vitro* experiments, these models do not directly describe *in vivo* properties of NDNBs, because the nonlinearity between the inhibition and the receptor occupancy causes the modulation of the resultant concentration-effect relationships of NDNBs.

Keywords: Anesthesia; Neuromuscular blockade; Receptor binding models; Nonlinear relationship

Background

Nondepolarizing neuromuscular blocking drugs (NDNBs) inhibit neuromuscular transmission by competing with acetylcholine (ACh) for binding sites at the post-

junctional nicotinic acetylcholine receptors (AChRs). They are widely used during general anesthesia to produce muscle relaxation for facilitating tracheal intubation and for providing optimal surgical working conditions [1]. To describe *in vivo* properties of NDNBs and to understand the molecular mechanisms behind clinical observations, many *in vitro* studies have been conducted (see e.g., [2–10]). In particular, in [7, 10], *in vitro* experiments have been conducted through macroscopic current recordings from outside-out patches of BOSC23 cells or Xenopus oocytes where human adult (rather than mouse adult or embryonic) muscle-type AChRs were expressed. In [7], synergistic effects of pairs of NDNBs have been studied. Although it successfully identified evidence for synergy between many pairs of NDNBs at the receptor level, not all the results correlated with synergism observed *in vivo*. In [9, 10], it was found that the IC_{50}, the drug concentration needed to produce a 50 % inhibition of the ACh-induced current, decreases with the increase in the concentration of ACh. Although it was concluded in [9, 10] that this demonstrated the existence of a noncompetitive action of NDNBs, some researchers raised concerns [11] over the insufficiency in quantitative analysis to draw the conclusion. Thus, more investigations and considerations are needed to describe the clinical observations and to clarify underlying mechanisms of inhibition based on *in vitro* experimental results.

While there are several measures identifying *in vitro* properties of NDNBs, potency [12] is one of the most widely used measures for studying NDNBs. It is usually quantified by IC_{50} estimated by regression analysis using the Hill equation for the relative current I_{antag}/I_0 given by

$$\frac{I_{\mathrm{antag}}}{I_0} = \frac{{IC_{50}}^{n_{\mathrm{H}}}}{{IC_{50}}^{n_{\mathrm{H}}} + [\mathrm{D}]^{n_{\mathrm{H}}}}, \tag{1}$$

where I_0 and I_{antag} stand for the currents measured in the absence and presence of the drugs, respectively. The parameter n_{H} stands for the Hill coefficient, and [D] for the drug concentration. Also, affinity [12], which is defined as the extent or fraction of drug binding to receptors at any given drug concentration, is used for characterizing the strength of the binding of a ligand to its receptors. In [4–8], the relative current versus concentration curves were analyzed based on the two-site receptor binding model given by the following equation:

$$\frac{I_{\mathrm{antag}}}{I_0} = \frac{K_{\mathrm{D1}}K_{\mathrm{D2}}}{K_{\mathrm{D1}}K_{\mathrm{D2}} + K_{\mathrm{D1}}[\mathrm{D}] + K_{\mathrm{D2}}[\mathrm{D}] + [\mathrm{D}]^2}, \tag{2}$$

where K_{D1} and K_{D2} stand for the dissociation equilibrium constants for NDNBs binding to the first and second sites of an AChR, respectively. Since the right-hand side of Eq. (2) represents the fraction of free receptors, i.e., the fraction of receptors that are not occupied by the drugs, the model (2) implies that the potency of an NDNB can be completely characterized by the affinity of the drug. However, in general, there may exist other factors that determine the potency of a drug. The underlying assumption for the use of the model (2) is that the inhibition, i.e. the effect of an NDNB, is proportional to the receptor occupancy by the drug. While the model (2) has been statistically tested in [4–8], the key factors affecting the

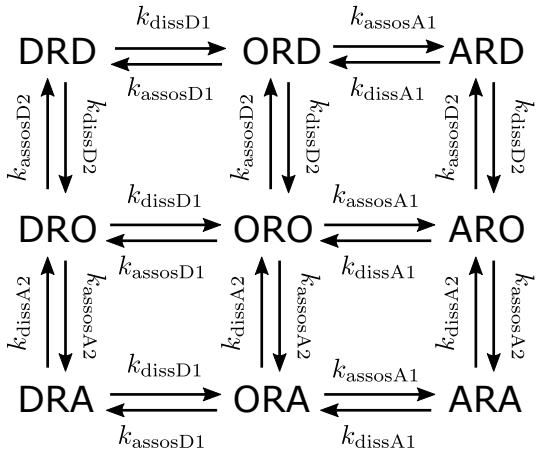

Figure 1 Diagram of the interactions between acetylcholine (A), NDNB (D), and the postsynaptic receptor (R). The complexes formed by binding of ACh and NDNB to AChR are represented by 3-letter symbols, where the first and last letters denote the first and second ligands occupying the sites 1 and 2, respectively. The complex ARA represents the activated AChR.

validity of this assumption have not been fully discussed in literature, and it has not been examined if the assumption holds *in vivo*.

The purpose of this study is to explore the *in vivo* relationship between the inhibition and the receptor occupancy by an NDNB and to draw implications on how *in vitro* experimental results can be used to discuss the *in vivo* pharmacologic properties of NDNBs. An ordinary differential equation model developed in [13] is employed to simulate physiologic processes of the activation of receptors by acetylcholine (ACh) as well as inhibition by an NDNB. Based on the model, we examine the conditions under which the relationship between inhibition and receptor occupancy becomes nonlinear and discuss its clinically relevant implications.

Methods

Model of competition between acetylcholine and NDNB

At the neuromuscular junction, electrical impulses from motor nerve cause the release of transmitter, ACh, to the synaptic cleft. Then, part of the released ACh molecules bind to AChRs on the muscle membrane and results in a change in the conductance of the membrane due to the channel opening. This change causes movement of ions into the muscle cell that produces an action potential spreading over the surfaces of skeletal muscle fibers and causing muscle contraction. NDNBs act by competing with ACh for binding to the two sites of an AChR and preventing changes in the membrane conductance. This paper uses the model developed in [13] to describe the competition between ACh and NDNB molecules for binding to AChRs. The complexes formed by binding of ACh, denoted by A, and NDNB, by D, to AChR, by R, are represented by 3-letter symbols as shown in Fig. 1. The first and last letters denote the first and second ligands occupying the sites 1 and 2, respectively, and the middle letter represents the receptor R. Unoccupied sites are denoted by O, and ORO stands for free AChR. The kinetics of ACh and NDNB are represented using association rate constants $k_{\mathrm{assocA}i}$ and $k_{\mathrm{assocD}i}$, for site $\#i$ ($i = 1, 2$), respectively. Similarly, $k_{\mathrm{dissA}i}$ and $k_{\mathrm{dissD}i}$ stand for the dissociation rate

constants for ACh and NDNB. Then, the concentrations of the eight complexes, e.g. [ARA] and [DRD], and of free ACh, [A], can be calculated as a function of time by solving the following ordinary differential equations [13]:

$$\begin{aligned}\frac{\mathrm{d}}{\mathrm{d}t}[\mathrm{A}] =& -k_{\mathrm{hydrolysis}}[\mathrm{A}] \\ &+ k_{\mathrm{dissA1}}([\mathrm{ARA}]+[\mathrm{ARD}]+[\mathrm{ARO}]) \\ &- k_{\mathrm{assocA1}}[\mathrm{A}]([\mathrm{ORA}]+[\mathrm{ORD}]+[\mathrm{ORO}]) \\ &+ k_{\mathrm{dissA2}}([\mathrm{ARA}]+[\mathrm{DRA}]+[\mathrm{ORA}]) \\ &- k_{\mathrm{assocA2}}[\mathrm{A}]([\mathrm{ARO}]+[\mathrm{DRO}]+[\mathrm{ORO}]), \end{aligned} \tag{3a}$$

$$\begin{aligned}\frac{\mathrm{d}}{\mathrm{d}t}[\mathrm{ARA}] =& k_{\mathrm{assocA1}}[\mathrm{ORA}][\mathrm{A}] - k_{\mathrm{dissA1}}[\mathrm{ARA}] \\ &+ k_{\mathrm{assocA2}}[\mathrm{ARO}][\mathrm{A}] - k_{\mathrm{dissA2}}[\mathrm{ARA}], \end{aligned} \tag{3b}$$

$$\begin{aligned}\frac{\mathrm{d}}{\mathrm{d}t}[\mathrm{DRD}] =& k_{\mathrm{assocD1}}[\mathrm{ORD}][\mathrm{D}] - k_{\mathrm{dissD1}}[\mathrm{DRD}] \\ &+ k_{\mathrm{assocD2}}[\mathrm{DRO}][\mathrm{D}] - k_{\mathrm{dissD2}}[\mathrm{DRD}], \end{aligned} \tag{3c}$$

$$\begin{aligned}\frac{\mathrm{d}}{\mathrm{d}t}[\mathrm{ARD}] =& k_{\mathrm{assocA1}}[\mathrm{ORD}][\mathrm{A}] - k_{\mathrm{dissA1}}[\mathrm{ARD}] \\ &+ k_{\mathrm{assocD2}}[\mathrm{ARO}][\mathrm{D}] - k_{\mathrm{dissD2}}[\mathrm{ARD}], \end{aligned} \tag{3d}$$

$$\begin{aligned}\frac{\mathrm{d}}{\mathrm{d}t}[\mathrm{DRA}] =& k_{\mathrm{assocD1}}[\mathrm{ORA}][\mathrm{D}] - k_{\mathrm{dissD1}}[\mathrm{DRA}] \\ &+ k_{\mathrm{assocA2}}[\mathrm{DRO}][\mathrm{A}] - k_{\mathrm{dissA2}}[\mathrm{DRA}], \end{aligned} \tag{3e}$$

$$\begin{aligned}\frac{\mathrm{d}}{\mathrm{d}t}[\mathrm{ARO}] =& k_{\mathrm{assocA1}}[\mathrm{ORO}][\mathrm{A}] - k_{\mathrm{dissA1}}[\mathrm{ARO}] \\ &+ k_{\mathrm{dissA2}}[\mathrm{ARA}] - k_{\mathrm{assocA2}}[\mathrm{ARO}][\mathrm{A}] \\ &+ k_{\mathrm{dissD2}}[\mathrm{ARD}] - k_{\mathrm{assocD2}}[\mathrm{ARO}][\mathrm{D}], \end{aligned} \tag{3f}$$

$$\begin{aligned}\frac{\mathrm{d}}{\mathrm{d}t}[\mathrm{ORA}] =& k_{\mathrm{assocA2}}[\mathrm{ORO}][\mathrm{A}] - k_{\mathrm{dissA2}}[\mathrm{ORA}] \\ &+ k_{\mathrm{dissA1}}[\mathrm{ARA}] - k_{\mathrm{assocA1}}[\mathrm{ORA}][\mathrm{A}] \\ &+ k_{\mathrm{dissD1}}[\mathrm{DRA}] - k_{\mathrm{assocD1}}[\mathrm{ORA}][\mathrm{D}], \end{aligned} \tag{3g}$$

$$\begin{aligned}\frac{\mathrm{d}}{\mathrm{d}t}[\mathrm{DRO}] =& k_{\mathrm{assocD1}}[\mathrm{ORO}][\mathrm{D}] - k_{\mathrm{dissD1}}[\mathrm{DRO}] \\ &+ k_{\mathrm{dissD2}}[\mathrm{DRD}] - k_{\mathrm{assocD2}}[\mathrm{DRO}][\mathrm{D}] \\ &+ k_{\mathrm{dissA2}}[\mathrm{DRA}] - k_{\mathrm{assocA2}}[\mathrm{DRO}][\mathrm{A}], \end{aligned} \tag{3h}$$

$$\begin{aligned}\frac{\mathrm{d}}{\mathrm{d}t}[\mathrm{ORD}] =& k_{\mathrm{assocD2}}[\mathrm{ORO}][\mathrm{D}] - k_{\mathrm{dissD2}}[\mathrm{ORD}] \\ &+ k_{\mathrm{dissD1}}[\mathrm{DRD}] - k_{\mathrm{assocD1}}[\mathrm{ORD}][\mathrm{D}] \\ &+ k_{\mathrm{dissA1}}[\mathrm{ARD}] - k_{\mathrm{assocA1}}[\mathrm{ORD}][\mathrm{A}], \end{aligned} \tag{3i}$$

where [D] stands for the concentration of NDNB at the effect site, and $k_{\mathrm{hydrolysis}}$ for the rate constant of hydrolysis of ACh by acetylcholinesterase. The concentration [ORO] of the unoccupied AChR is given by

$$\begin{aligned}[\mathrm{ORO}] =& [\mathrm{R}]_{\mathrm{total}} - [\mathrm{ARA}] - [\mathrm{DRD}] - [\mathrm{ARD}] - [\mathrm{DRA}] \\ &- [\mathrm{ARO}] - [\mathrm{ORA}] - [\mathrm{DRO}] - [\mathrm{ORD}], \end{aligned} \tag{4}$$

Table 1 Setting of parameters for numerical simulation in base case

symbol	meaning	value
$[\mathrm{R}]_{\mathrm{total}}$	Concentration of AChRs in the synaptic cleft	$7.75 \times 10^{-5}\,\mathrm{M}$ [13]
$[\mathrm{A}]_{\mathrm{init}}$	Initial concentration of ACh immediately after the stimulus	$7.75 \times 10^{-6}\,\mathrm{M}$ [13]
$k_{\mathrm{hydrolysis}}$	Rate constant of hydrolysis of ACh	$1.2 \times 10^{4}\,\mathrm{s}^{-1}$ [13]
k_{dissA1}	Dissociation rate constant for ACh with site1 of AChR	$1.8 \times 10^{4}\,\mathrm{s}^{-1}$ [14]
k_{dissA2}	Dissociation rate constant for ACh with site2 of AChR	$1.8 \times 10^{4}\,\mathrm{s}^{-1}$ [14]
k_{assocA1}	Association rate constant for ACh with site1 of AChR *	$1.1 \times 10^{8}\,\mathrm{M}^{-1}\,\mathrm{s}^{-1}$ [14]
k_{assocA2}	Association rate constant for ACh with site2 of AChR *	$1.1 \times 10^{8}\,\mathrm{M}^{-1}\,\mathrm{s}^{-1}$ [14]
k_{dissD1}	Dissociation rate constant for NDNB with site1 of AChR *	$10\,\mathrm{s}^{-1}$ [4, 5]
k_{dissD2}	Dissociation rate constant for NDNB with site2 of AChR *	$10\,\mathrm{s}^{-1}$ [4, 5]
k_{assocD1}	Association rate constant for NDNB with site1 of AChR *	$1.0 \times 10^{8}\,\mathrm{M}^{-1}\,\mathrm{s}^{-1}$ [4, 5]
k_{assocD2}	Association rate constant for NDNB with site2 of AChR *	$1.0 \times 10^{8}\,\mathrm{M}^{-1}\,\mathrm{s}^{-1}$ [4, 5]

∗ These dissociation and association rate constants are varied in numerical analysis

where $[\mathrm{R}]_{\mathrm{total}}$ stands for the concentration of the post-junctional AChRs in the synaptic cleft.

Here we provide an example of simulation results of the model (3). The setting of the parameters is shown in Table 1. Following [13], the concentration $[\mathrm{R}]_{\mathrm{total}}$ of AChRs was calculated using the number of AChRs at the end plates of human deltoid muscle and the volume of the synaptic cleft, and the initial concentration $[\mathrm{A}]_{\mathrm{init}}$ of the free ACh calculated by assuming that the number of ACh molecules released is one tenth of the number of AChRs. The rate constant $k_{\mathrm{hydrolysis}}$ was determined such that the half-life of free ACh becomes $58\,\mu$s as calculated in [13]. The dissociation and association rate constants for ACh were tentatively set to the values obtained in [14] from experiments using mouse adult AChRs. Similarly, the rate constants for NDNBs were set to tentative values based on experiments in [4, 5] using mouse embryonic and adult AChRs. Since the values of these rate constants may be different between human and mouse AChRs, these constants will be varied in a systematic way. Figure 2 shows the time courses of the concentrations of free ACh, [A], and of the activated AChRs, [ARA], after the arrival of an electrical impulse from motor nerve and the release of ACh at $t = 0$. The initial concentrations for the eight complexes at $t = 0$ were defined by the steady state concentrations before the release of ACh. The concentration of the NDNB was set to one of $[\mathrm{D}] = 0$, $3.0 \times 10^{-8}\,\mathrm{M}$, and $1.0 \times 10^{-7}\,\mathrm{M}$. As shown in the upper panel of Fig. 2, the concentration of ACh rapidly decreases due to the hydrolysis of ACh by acetylcholinesterase and binding of ACh to AChRs. The time course of the complex ARA is shown in the lower panel of Fig. 2. The concentration [ARA] raises rapidly and after reaching the peak at around $t = 0.06\,\mathrm{ms}$, returns to the steady state. The highest [ARA], denoted by $[\mathrm{ARA}]_{\mathrm{max}}$, is attained in the absence of NDNB, i.e., $[\mathrm{D}] = 0$, and the peak concentration $[\mathrm{ARA}]_{\mathrm{peak}}$ decreases with the increase in the concentration of [D]. With this model, the effect of an NDNB can be quantified by a fraction of activated AChRs given by $[\mathrm{ARA}]_{\mathrm{peak}}/[\mathrm{ARA}]_{\mathrm{max}}$. This definition corresponds to the relative current I_{antag}/I_0 used in *in vitro* experiments under the assumption that the membrane conductance is proportional to the number of activated AChRs, i.e. the number of opened ion channels:

$$\frac{I_{\mathrm{antag}}}{I_0} = \frac{[\mathrm{ARA}]_{\mathrm{peak}}}{[\mathrm{ARA}]_{\mathrm{max}}}. \tag{5}$$

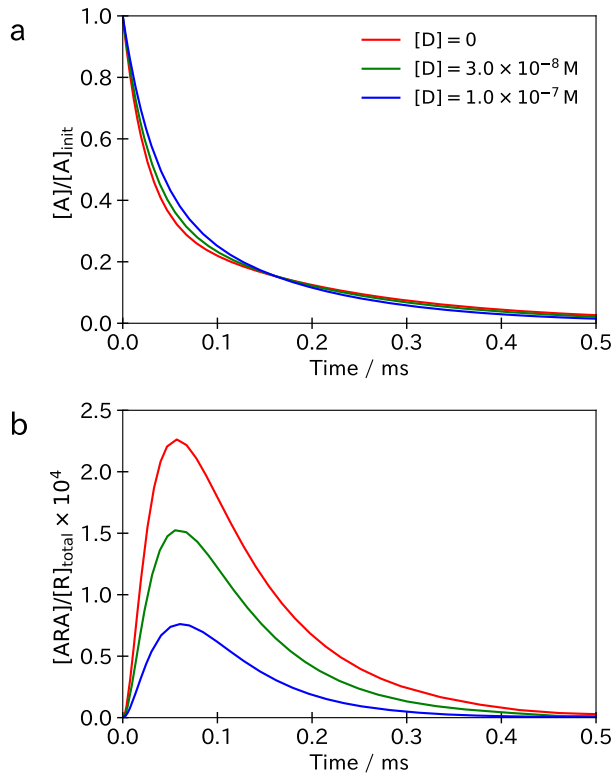

Figure 2 An example of simulation results of the model (3). **a** The time course of the concentration [A] of free ACh. **b** The time course of the concentration [ARA] of the complex ARA representing the activated AChRs.

Theoretical analysis of the competition model

To conduct the subsequent numerical analysis in a systematic way, here we theoretically analyze the model (3). Specifically, we derive a dimensionless representation of the model based on the technique of scaling [15] and perform model-order reduction based on singular perturbation theory [16,17]. As a result, it will be shown that it is possible to reduce the number of independent parameters in the model. First, the scaling of the model (3) can be done by introducing dimensionless variables. For example, a dimensionless time τ and a concentration of ACh, x_{A}, can be defined as

$$\tau := t \cdot k_{\mathrm{hydrolysis}}, \quad x_{\mathrm{A}} := \frac{[\mathrm{A}]}{K_{\mathrm{A1}}}, \tag{6}$$

where K_{A1} stands for the dissociation equilibrium constant for ACh with the site #1 given by $k_{\mathrm{dissA1}}/k_{\mathrm{assocA1}}$. Dimensionless variables x_{ARA} and x_{DRD} for the concentrations of the complex ARA and DRD are given by

$$x_{\mathrm{ARA}} := \frac{[\mathrm{ARA}]}{[\mathrm{R}]_{\mathrm{total}}}, \quad x_{\mathrm{DRD}} := \frac{[\mathrm{DRD}]}{[\mathrm{R}]_{\mathrm{total}}}. \tag{7}$$

Similarly, the dimensionless variables x_{ARD}, x_{DRA}, x_{ARO}, x_{ORA}, x_{DRO}, and x_{ORD} for the remaining six complexes can be defined by dividing by $[\mathrm{R}]_{\mathrm{total}}$. The model

(3) can be rewritten in a dimensionless form by using these variables (see Appendix for the resultant equations). For example, the time courses of the concentrations of free ACh, ARA and DRD are given by

$$\begin{aligned}\frac{\mathrm{d}}{\mathrm{d}\tau}x_{\mathrm{A}} =& - x_{\mathrm{A}} + \kappa_{\mathrm{A1}}\lambda_{\mathrm{A1}}\{x_{\mathrm{ARA}} + x_{\mathrm{ARD}} + x_{\mathrm{ARO}} \\ & - x_{\mathrm{A}}(x_{\mathrm{ORA}} + x_{\mathrm{ORD}} + x_{\mathrm{ORO}})\} \\ & + \kappa_{\mathrm{A2}}\{\lambda_{\mathrm{A1}}(x_{\mathrm{ARA}} + x_{\mathrm{DRA}} + x_{\mathrm{ORA}}) \\ & - \lambda_{\mathrm{A2}}x_{\mathrm{A}}(x_{\mathrm{ARO}} + x_{\mathrm{DRO}} + x_{\mathrm{ORO}})\}, \end{aligned} \tag{8}$$

$$\frac{\mathrm{d}}{\mathrm{d}\tau}x_{\mathrm{ARA}} = \kappa_{\mathrm{A1}}\left(x_{\mathrm{ORA}}x_{\mathrm{A}} - x_{\mathrm{ARA}}\right) + \kappa_{\mathrm{A2}}\left(\mu_{\mathrm{A}}x_{\mathrm{ARO}}x_{\mathrm{A}} - x_{\mathrm{ARA}}\right), \tag{9}$$

$$\frac{\mathrm{d}}{\mathrm{d}\tau}x_{\mathrm{DRD}} = \kappa_{\mathrm{D1}}\left(x_{\mathrm{ORD}}\delta - x_{\mathrm{DRD}}\right) + \kappa_{\mathrm{D2}}\left(\mu_{\mathrm{D}}x_{\mathrm{ORD}}\delta - x_{\mathrm{DRD}}\right), \tag{10}$$

where κ_{A1}, κ_{A2}, κ_{D1} and κ_{D2} are the dimensionless parameters representing the rates of the both dissociation and association of the ligands given by

$$\begin{aligned}\kappa_{\mathrm{A1}} &:= \frac{k_{\mathrm{dissA1}}}{k_{\mathrm{hydrolysis}}}, \quad \kappa_{\mathrm{A2}} := \frac{k_{\mathrm{dissA2}}}{k_{\mathrm{hydrolysis}}}, \\ \kappa_{\mathrm{D1}} &:= \frac{k_{\mathrm{dissD1}}}{k_{\mathrm{hydrolysis}}}, \quad \kappa_{\mathrm{D2}} := \frac{k_{\mathrm{dissD2}}}{k_{\mathrm{hydrolysis}}}, \end{aligned} \tag{11}$$

and λ_{A1}, λ_{A2}, and $\mu_{\mathrm{A}}$are the dimensionless parameters representing affinities of ACh to the binding sites of the AChR given by

$$\lambda_{\mathrm{A1}} := \frac{[\mathrm{R}]_{\mathrm{total}}}{K_{\mathrm{A1}}}, \quad \lambda_{\mathrm{A2}} := \frac{[\mathrm{R}]_{\mathrm{total}}}{K_{\mathrm{A2}}}, \quad \mu_{\mathrm{A}} := \frac{K_{\mathrm{A1}}}{K_{\mathrm{A2}}}, \tag{12}$$

with $K_{\mathrm{A2}} := k_{\mathrm{dissA2}}/k_{\mathrm{assocA2}}$, and finally, μ_{D} and δ are the dimensionless parameters representing the site-selectivity and concentration of NDNB, respectively, given by

$$\mu_{\mathrm{D}} := \frac{K_{\mathrm{D1}}}{K_{\mathrm{D2}}}, \quad \delta := \frac{[\mathrm{D}]}{K_{\mathrm{D1}}}, \tag{13}$$

with $K_{\mathrm{D1}} := k_{\mathrm{dissD1}}/k_{\mathrm{assocD1}}$ and $K_{\mathrm{D2}} := k_{\mathrm{dissD2}}/k_{\mathrm{assocD2}}$. Note that due to the scaling performed here, the number of parameters characterizing the properties of NDNB can be reduced from four to three: from (k_{dissD1}, k_{asoocD1}, k_{dissD2}, k_{assocD2}) to (κ_{D1}, κ_{D2}, μ_{D}).

Furthermore, the order of the model can be reduced using the technique of singular perturbation [16,17] based on an inherent multiple-timescale property of the model. Such a multi-scale property arises when the dissociation rate constants k_{dissD1} and k_{dissD2} of an NDNB are much smaller than other rate constants such as k_{dissA1}, k_{dissA2} and $k_{\mathrm{hydrolysis}}$, and this is the case for several clinically used NDNBs. For cisatracurium, the dissociation rate constants are reported in [5] as $13\,\mathrm{s}^{-1}$ and $34\,\mathrm{s}^{-1}$ for mouse adult and embryonic AChRs, respectively. Also, these values are reported in [4] as $2.1\,\mathrm{s}^{-1}$ and $5.9\,\mathrm{s}^{-1}$ for (+)-tubocurarine and pancuronium, respectively. Whereas, the dissociation rate constants of ACh and the rate constant of hydrolysis are estimated as $18\,000\,\mathrm{s}^{-1}$ and $12\,000\,\mathrm{s}^{-1}$, respectively [13, 14]. Under the assumption that k_{dissD1} and k_{dissD2} are small, a simplified model can be

derived by considering the limit κ_{D1}, $\kappa_{\mathrm{D2}} \to 0$. Under the limit operation, the following equations can be derived (they can be easily verified from the dimensionless equations shown in Appendix):

$$\frac{\mathrm{d}}{\mathrm{d}\tau}x_{\mathrm{DRD}} = \frac{\mathrm{d}}{\mathrm{d}\tau}(x_{\mathrm{ORD}} + x_{\mathrm{ARD}}) = \frac{\mathrm{d}}{\mathrm{d}\tau}(x_{\mathrm{DRO}} + x_{\mathrm{DRA}}) = 0. \tag{14}$$

Thus, the values of x_{DRD}, $x_{\mathrm{ORD}} + x_{\mathrm{ARD}}$ and $x_{\mathrm{DRO}} + x_{\mathrm{DRA}}$ do not change in the reduced-order model, or almost unchanged in the original model (3), from their initial values at $\tau = 0$. When the initial conditions are defined by the steady state concentrations under a given value of δ, the initial values of x_{DRD}, x_{ORD}, x_{DRO}, x_{ARD} and x_{DRA} are given by

$$x_{\mathrm{DRD}}|_{\tau=0} = O_{\mathrm{DRD}}(\delta) := \frac{\mu_{\mathrm{D}}\delta^2}{(1+\delta)(1+\mu_{\mathrm{D}}\delta)}, \tag{15a}$$

$$x_{\mathrm{ORD}}|_{\tau=0} = O_{\mathrm{ORD}}(\delta) := \frac{\mu_{\mathrm{D}}\delta}{(1+\delta)(1+\mu_{\mathrm{D}}\delta)}, \tag{15b}$$

$$x_{\mathrm{DRO}}|_{\tau=0} = O_{\mathrm{DRO}}(\delta) := \frac{\delta}{(1+\delta)(1+\mu_{\mathrm{D}}\delta)}, \tag{15c}$$

$$x_{\mathrm{ARD}}|_{\tau=0} = x_{\mathrm{DRA}}|_{\tau=0} = 0 \tag{15d}$$

where O_{DRD}, O_{ORD} and O_{DRO} stand for the fractions of the complex DRD, ORD, and DRO, respectively, at the steady state. Also, the total occupancy O_{total} of the AChRs by the NDNB is given by

$$O_{\mathrm{total}}(\delta) := O_{\mathrm{DRD}}(\delta) + O_{\mathrm{ORD}}(\delta) + O_{\mathrm{DRO}}(\delta). \tag{16}$$

By using the equations from (14) to (16), the model (3) can be reduced to the following form:

$$\begin{aligned}\frac{\mathrm{d}}{\mathrm{d}\tau}x_{\mathrm{A}} = &-x_{\mathrm{A}} + \kappa_{\mathrm{A1}}\lambda_{\mathrm{A1}}\{x_{\mathrm{ARA}} - x_{\mathrm{A}}(O_{\mathrm{ORD}}(\delta) - x_{\mathrm{ARD}})\} \\ &+ \kappa_{\mathrm{A2}}\lambda_{\mathrm{A2}}\{x_{\mathrm{ARA}} - x_{\mathrm{A}}(O_{\mathrm{DRO}}(\delta) - x_{\mathrm{DRA}})\} \\ &+ \kappa_{\mathrm{A1}}\lambda_{\mathrm{A1}}\{x_{\mathrm{ARD}} + x_{\mathrm{ARO}} - x_{\mathrm{A}}(1 - x_{\mathrm{ARA}} - x_{\mathrm{ARO}} - O_{\mathrm{total}}(\delta))\} \\ &+ \kappa_{\mathrm{A2}}\lambda_{\mathrm{A2}}\{x_{\mathrm{DRA}} + x_{\mathrm{ORA}} - x_{\mathrm{A}}(1 - x_{\mathrm{ARA}} - x_{\mathrm{ORA}} - O_{\mathrm{total}}(\delta))\},\end{aligned} \tag{17a}$$

$$\frac{\mathrm{d}}{\mathrm{d}\tau}x_{\mathrm{ARA}} = \kappa_{\mathrm{A1}}\left(x_{\mathrm{ORA}}x_{\mathrm{A}} - x_{\mathrm{ARA}}\right) + \kappa_{\mathrm{A2}}\left(\mu_{\mathrm{A}}x_{\mathrm{ARO}}x_{\mathrm{A}} - x_{\mathrm{ARA}}\right), \tag{17b}$$

$$\begin{aligned}\frac{\mathrm{d}}{\mathrm{d}\tau}x_{\mathrm{ARO}} = &\kappa_{\mathrm{A1}}\left\{x_{\mathrm{A}}(1 - x_{\mathrm{ARA}} - x_{\mathrm{ARO}} - x_{\mathrm{ORA}} - O_{\mathrm{total}}(\delta)) - x_{\mathrm{ARO}}\right\} \\ &+ \kappa_{\mathrm{A2}}\left(x_{\mathrm{ARA}} - \mu_{\mathrm{A}}x_{\mathrm{ARO}}x_{\mathrm{A}}\right),\end{aligned} \tag{17c}$$

$$\begin{aligned}\frac{\mathrm{d}}{\mathrm{d}\tau}x_{\mathrm{ORA}} = &\kappa_{\mathrm{A2}}\left\{\mu_{\mathrm{A}}x_{\mathrm{A}}(1 - x_{\mathrm{ARA}} - x_{\mathrm{ARO}} - x_{\mathrm{ORA}} - O_{\mathrm{total}}(\delta)) - x_{\mathrm{ORA}}\right\} \\ &+ \kappa_{\mathrm{A1}}\left(x_{\mathrm{ARA}} - x_{\mathrm{ORA}}x_{\mathrm{A}}\right),\end{aligned} \tag{17d}$$

$$\frac{\mathrm{d}}{\mathrm{d}\tau}x_{\mathrm{ARD}} = \kappa_{\mathrm{A1}}\left\{x_{\mathrm{A}}(O_{\mathrm{ORD}}(\delta) - x_{\mathrm{ARD}}) - x_{\mathrm{ARD}}\right\}, \tag{17e}$$

$$\frac{\mathrm{d}}{\mathrm{d}\tau}x_{\mathrm{DRA}} = \kappa_{\mathrm{A2}}\left\{\mu_{\mathrm{A}}x_{\mathrm{A}}(O_{\mathrm{DRO}}(\delta) - x_{\mathrm{DRA}}) - x_{\mathrm{DRA}}\right\}. \tag{17f}$$

In the reduced-order model (17), it can be seen that the number of independent parameters regarding NDNBs is only one, that is the properties of NDNBs are completely characterized by the single parameter μ_{D}, since the parameters κ_{D1} and κ_{D2} vanish due to the limit operation. This fact implies that even in simulations of the original model (3), the results will be almost unchanged if the parameter μ_{D} kept constant and the parameters κ_{D1} and κ_{D2} are small. This facilitates the numerical analysis of the original model (3) by varying the parameters of the model in a systematic way as demonstrated in the rest of the paper. Furthermore, it can be seen that the parameter δ representing the dimensionless concentration of the NDNB affects the dynamics governed by the model (17) through the partial and total occupancy O_{ORD}, O_{DRO}, and O_{total} at the steady state. While the two-site model (2) is based on the assumption that the inhibition is proportional to the total occupancy O_{total}, the relationship between inhibition and the occupancy estimated by the models (3) or (17) is also affected by the partial occupancy O_{ORD} and O_{DRO}.

Method of numerical analysis on the relationship between inhibition and receptor occupancy

The relationship between the inhibition and the receptor occupancy by an NDNB is studied via numerical simulations of the original model (3). To visualize the results, the fraction of activated AChRs given by $[\mathrm{ARA}]_{\mathrm{peak}}/[\mathrm{ARA}]_{\mathrm{max}}$ is calculated under various concentrations of the NDNB (100 values between $[\mathrm{D}] = 1.0 \times 10^{-14}\,\mathrm{M}$ and $1.0 \times 10^{-5}\,\mathrm{M}$ that are spaced equidistantly on a logarithmic scale, and $[\mathrm{D}] = 0$) and plotted versus the total occupancy O_{total}. For calculating the peak concentration of ARA, the ordinary differential equation model (3) is numerically solved using the Fortran solver LSODA provided by the python package SciPy (Version 1.5.2).

The parameters of the model (3) are varied in a systematic way based on information provided by literature and the findings of the theoretical analysis as explained in the following. First, we investigate the effect of varying the kinetic constants for ACh and NDNB. For ACh, the values of k_{dissA1}, k_{dissA2}, k_{assocA1}, and k_{assocA2} presented in Table 1 were determined by experiments using mouse adult AChRs. However, it is known that the EC_{50}, the concentration of ACh where the half of the AChRs are activated, for human adult AChRs is smaller than that for mouse adult AChRs: $\mathrm{EC}_{50} = 8.48 \times 10^{-6}\,\mathrm{M}$ or $7.91 \times 10^{-6}\,\mathrm{M}$ for human adult AChRs [10] and $\mathrm{EC}_{50} = 1.6 \times 10^{-5}\,\mathrm{M}$ for mouse adult AChRs [14]. Since this implies that the affinity of ACh is different between human and mouse AChRs, we investigated the effect of varying the constants K_{A1} and K_{A2} by changing k_{assocA1} and k_{assocA2} while k_{dissA1} and k_{dissA2} kept constant. Furthermore, since it has been reported in [14] that the two binding sites of mouse adult AChR have similar affinities, we assume that it is also the case for human adult AChR and the parameters K_{A1} and K_{A2} are equal. Thus, we investigate the effect of varying the values of $K_{\mathrm{A1}} = K_{\mathrm{A2}} = K_{\mathrm{A}}$, which corresponds to $\kappa_{\mathrm{A1}} = \kappa_{\mathrm{A2}}$ and $\mu_{\mathrm{A}} = 1$. For the kinetic constants of an NDNB, the effect of varying the parameter μ_{D} is investigated, since this parameter completely characterizes the properties of the NDNB as far as the dissociation constants k_{dissD1} and k_{dissD2} are small enough. The value of parameter μ_{D} was assigned by changing the value of k_{assocD2}, while k_{dissD1}, k_{dissD2} and k_{assocD1} kept constant at the values shown in Table 1. Also, the values of the dissociation constants k_{dissD1}

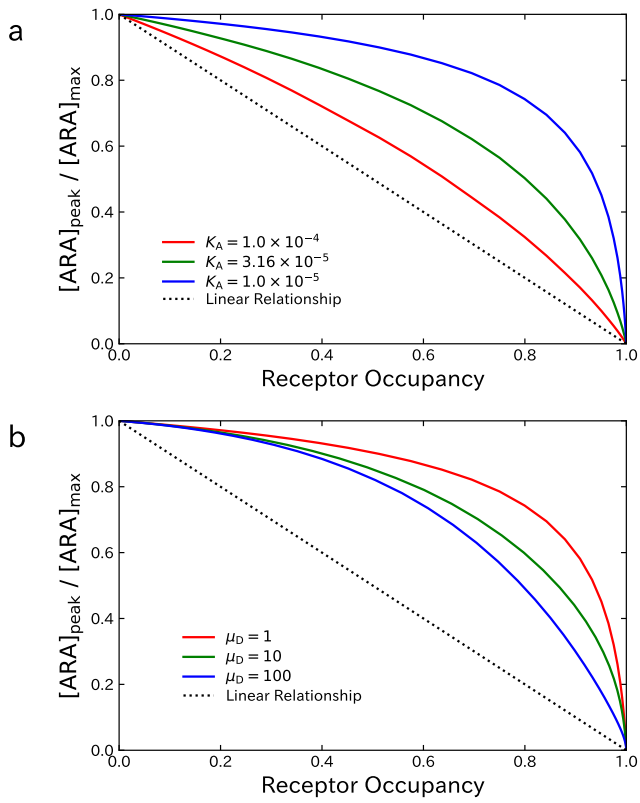

Figure 3 Effect of varying kinetic constants for ACh and NDNB on the relationship between the fraction of activated AChRs, $[\mathrm{ARA}]_{\mathrm{peak}}/[\mathrm{ARA}]_{\mathrm{max}}$, and the receptor occupancy O_{total}. **a** Results of varying the equilibrium dissociation constants for ACh under $K_{\mathrm{A}} = K_{\mathrm{A1}} = K_{\mathrm{A2}}$ ($\kappa_{\mathrm{A1}} = \kappa_{\mathrm{A2}}$ and $\mu_{\mathrm{A}} = 1$). **b** Results of varying the site-selectivity $\mu_{\mathrm{D}} = K_{\mathrm{D1}}/K_{\mathrm{D2}}$ of an NDNB.

and k_{dissD2} are varied to explore the difference between the original model (3) and the reduced-order model (17).

Furthermore, we examine the effect of varying the initial concentration $[\mathrm{A}]_{\mathrm{init}}$ representing the concentration of ACh immediately after the release of ACh at $t = 0$. It has been known that the number of ACh molecules released *in vivo* is one tenth of the number of AChRs at the synaptic cleft [13]. In this paper, following [13], the concentrations of AChRs and the initial ACh were set as $[\mathrm{R}]_{\mathrm{total}} = 7.75 \times 10^{-5}\,\mathrm{M}$ and $[\mathrm{A}]_{\mathrm{init}} = 7.75 \times 10^{-6}\,\mathrm{M}$, respectively. Under this setting, only a small fraction (at least less than one tenth) of the total receptor population will be activated *in vivo*. However, in many *in vitro* experiments, a quite high concentration of ACh is used [4–8] such that nearly 50 % (nearly EC_{50}) of the AChRs are activated or more than 90 % of AChRs are activated. Thus, we investigated the effect of varying $[\mathrm{A}]_{\mathrm{init}}$ in a wide range of concentrations from $[\mathrm{A}]_{\mathrm{init}} = 0.1 \times [\mathrm{R}]_{\mathrm{total}}$ to $10 \times [\mathrm{R}]_{\mathrm{total}}$.

Results

The upper panel of Fig. 3 shows the relationship between the fraction of activated AChRs given by $[\mathrm{ARA}]_{\mathrm{peak}}/[\mathrm{ARA}]_{\mathrm{max}}$ and the receptor occupancy O_{total} evaluated under various settings of the dissociation equilibrium constants for ACh. The values of $K_{\mathrm{A1}} = K_{\mathrm{A2}} = K_{\mathrm{A}}$ is one of $1.0 \times 10^{-4}\,\mathrm{M}$, $3.16 \times 10^{-5}\,\mathrm{M}$ and $1.0 \times 10^{-5}\,\mathrm{M}$, and

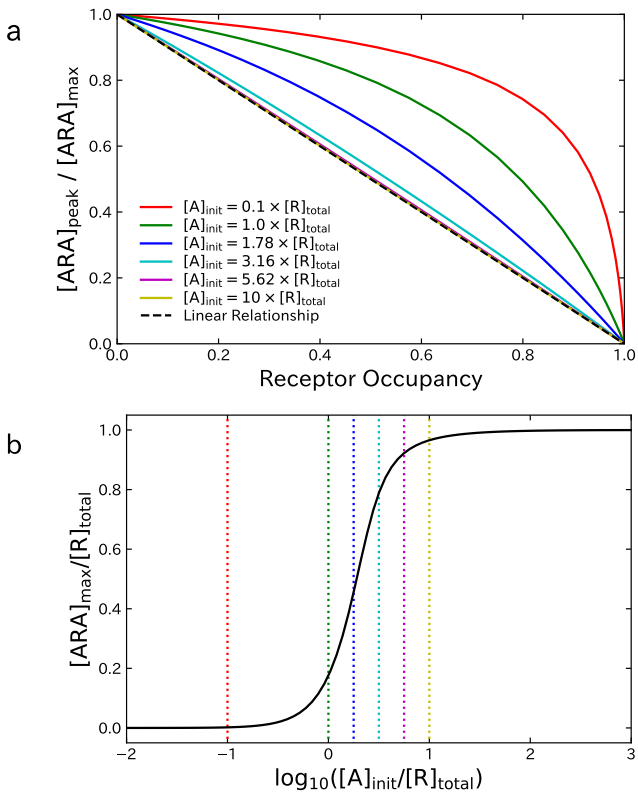

Figure 4 Effect of varying the initial concentration $[\mathrm{A}]_{\mathrm{init}}$ of ACh on the numerical results. **a** The relationship between the fraction of activated AChRs, $[\mathrm{ARA}]_{\mathrm{peak}}/[\mathrm{ARA}]_{\mathrm{max}}$, and the receptor occupancy O_{total} under various settings of $[\mathrm{A}]_{\mathrm{init}}$. **b** The concentration-effect relationship between the activated AChRs in the absence of NDNBs and the initial concentration $[\mathrm{A}]_{\mathrm{init}}$.

shown by *red*, *green* and *blue* lines, respectively. The dotted line in the figure shows the linear relationship corresponding to the model (2). The results clearly show that there are nonlinear relationships between $[\mathrm{ARA}]_{\mathrm{peak}}/[\mathrm{ARA}]_{\mathrm{max}}$ and O_{total} in all the cases. Furthermore, it can be confirmed that the extent of nonlinearity increases with the decrease in the equilibrium constant K_{A}. In the subsequent analyses, to highlight the effects of varying other parameters, we assigned the value of 1.0×10^{-5} M to K_{A}, where the extent of nonlinearity was most prominent. Then, the lower panel of Fig. 3 shows the results under various setting of μ_{D} representing the site-selectivity of an NDNB. The *red*, *green* and *blue* lines show the results for $\mu_{\mathrm{D}} = 1$, 10, and 100, respectively. It can be seen that the relationships between $[\mathrm{ARA}]_{\mathrm{peak}}/[\mathrm{ARA}]_{\mathrm{max}}$ and O_{total} are nonlinear in all the cases, and the extent of nonlinearity decreases with the increase in μ_{D}.

Next, the upper panel of Fig. 4 shows the relationship between the fraction of activated AChRs, $[\mathrm{ARA}]_{\mathrm{peak}}/[\mathrm{ARA}]_{\mathrm{max}}$, and the receptor occupancy O_{total} under various settings of the initial concentration of ACh, $[\mathrm{A}]_{\mathrm{init}}$. It can be seen from the figure that the extent of nonlinearity decreases with the increase in the initial concentration $[\mathrm{A}]_{\mathrm{init}}$. Interestingly, the relationship between $[\mathrm{ARA}]_{\mathrm{peak}}/[\mathrm{ARA}]_{\mathrm{max}}$ and O_{total} becomes almost linear when the value of $[\mathrm{A}]_{\mathrm{init}}$ is larger than $5.62 \times [\mathrm{R}]_{\mathrm{total}}$. To clarify the meaning of this result, the lower panel of Fig. 4 shows the concentration-

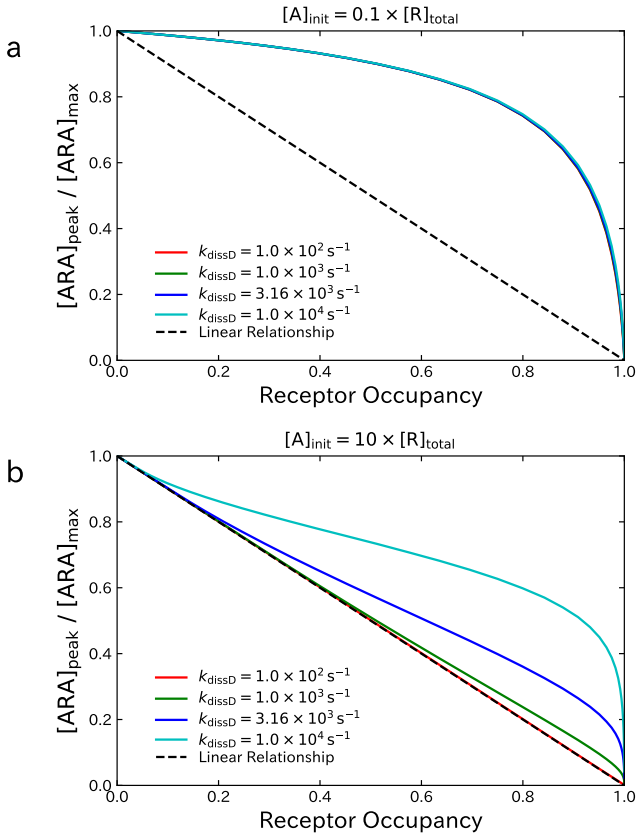

Figure 5 Effect of varying the dissociation rate constants k_{dissD1} and k_{kdissD2} on the relationship between the fraction of activated AChRs, $[\mathrm{ARA}]_{\mathrm{peak}}/[\mathrm{ARA}]_{\mathrm{max}}$, and the receptor occupancy O_{total}. **a** Results under the setting of $[\mathrm{A}]_{\mathrm{init}} = 0.1 \times [\mathrm{R}]_{\mathrm{total}}$ corresponding to *in vivo* concentration. **b** Results under the setting of $[\mathrm{A}]_{\mathrm{init}} = 10 \times [\mathrm{R}]_{\mathrm{total}}$ corresponding to *in vitro* concentration.

response relationship between the concentration $[\mathrm{A}]_{\mathrm{init}}$ and the activated AChRs $[\mathrm{ARA}]_{\mathrm{max}}$. Note that the $[\mathrm{ARA}]_{\mathrm{max}}$ is defined for each setting of $[\mathrm{A}]_{\mathrm{init}}$ as the highest [ARA] under various settings of the concentration of an NDNB, and it is attained in the absence of NDNB. At the setting of $[\mathrm{A}]_{\mathrm{init}} = 0.1 \times [\mathrm{R}]_{\mathrm{total}}$, which corresponds to the *in vivo* situation [13], only a fraction of AChRs are activated even in the absence of NDNBs, and result in a highly nonlinear relationship between $[\mathrm{ARA}]_{\mathrm{peak}}/[\mathrm{ARA}]_{\mathrm{max}}$ and O_{total}. However, at the setting of $[\mathrm{A}]_{\mathrm{init}} \geq 5.63 \times [\mathrm{R}]_{\mathrm{total}}$, more than 92 % of AChRs are activated in the absence of NDNB, and in this case, the relationship between $[\mathrm{ARA}]_{\mathrm{peak}}/[\mathrm{ARA}]_{\mathrm{max}}$ and O_{total} becomes linear.

Finally, the effect of varying the dissociation rate constants k_{dissD1} and k_{dissD2} of NDNB was examined under the setting of identical rate constants, i.e. $k_{\mathrm{dissD1}} = k_{\mathrm{dissD2}} = k_{\mathrm{dissD}}$. The upper panel of Fig. 5 shows the relationship between the fraction of activated AChRs, $[\mathrm{ARA}]_{\mathrm{peak}}/[\mathrm{ARA}]_{\mathrm{max}}$, and the receptor occupancy O_{total} under the setting of $[\mathrm{A}]_{\mathrm{init}} = 0.1 \times [\mathrm{R}]_{\mathrm{total}}$ corresponding to *in vivo* concentration. With this setting, the results are almost unchanged even when the rate constant k_{dissD} is as large as k_{dissA1}, k_{dissA2}, and $k_{\mathrm{hydrolysis}}$. The lower panel of Fig. 5 shows the results under the setting of $[\mathrm{A}]_{\mathrm{init}} = 10 \times [\mathrm{R}]_{\mathrm{total}}$ corresponding to *in vitro* con-

centration. In this case, it can be seen that the results are highly affected by the setting of the dissociation rate constant k_{dissD}. Furthermore, the relationships between $[\mathrm{ARA}]_{\mathrm{peak}}/[\mathrm{ARA}]_{\mathrm{max}}$ and O_{total} are no longer linear when the rate constant k_{dissD} becomes large even if the concentration $[\mathrm{A}]_{\mathrm{init}}$ is large.

Discussion

We theoretically and numerically investigated the relationship between inhibition and receptor occupancy by NDNBs. While the two-site receptor binding model (2), which assumes a linear relationship between the inhibition and the receptor occupancy by an NDNB, has been statistically tested in [4–8] for several *in vitro* experimental settings, it has not been studied in literature under which conditions the above assumption holds nor if the assumption remains valid *in vivo*. To consider these problems, an ordinary differential equation model developed in [13] was employed to simulate the physiologic processes of activation of receptors by ACh as well as inhibition by an NDNB. The theoretical analysis performed in this paper clarified that under the assumption that the dissociation rate constants for an NDNB are small and with an appropriate nondimensionalization, the characteristics of an NDNB can be completely determined by a single parameter μ_{D} representing the site-selectivity of the NDNB for two binding sites of AChRs. We then performed numerical analysis of the model by plotting the fractional amounts of the activated AChRs as a function of the receptor occupancy. The numerical results show that under a setting of parameters reflecting *in vivo* environment, there is a nonlinear relationship between the inhibition and the receptor occupancy, indicating limitation of the applicability of the receptor binding model. Furthermore, it has been shown that the extent of nonlinearity depends on the parameters representing kinetic constants for ACh or NDNBs and the concentration of ACh.

Regarding the nonlinear relationship between the effect and the receptor occupancy by an NDNB, it has been well known that the twitch strength (the degree of muscle contraction) observed *in vivo* is not proportional to the receptor occupancy due to the high margin of safety [18]. The origin of the safety margin is a copious density of AChRs on the post-synaptic membrane and the fact that only a small fraction of AChRs needs to be activated to trigger the occurrence of an action potential and the contraction of the associated muscle fiber. Thus, the nonlinearity due to the safety margin means that the response of muscle fiber is not proportional to the fraction of activated AChRs, and the extent of nonlinearity would not be affected by the properties of an NDNB. However, this paper focused on the nonlinearity in the relationship between the receptor occupancy and the fraction of activated AChRs, and the extent of nonlinearity is affected by the properties of an NDNB. In particular, it has been revealed in this paper that the effect of an NDNB on the extent of nonlinearity can be characterized by a single parameter μ_{D} representing the site-selectivity of the NDNB.

Our finding that the extent of nonlinearity is affected by the concentration of ACh provides an important implication to interpret *in vitro* experimental results as follows. In [9, 10], it was found that the IC_{50} for several clinically used NDNBs, cis-atracrium, rocuronium, and vecronium, decreased with the increase in the concentration of ACh. With these results, it was concluded in [9, 10, 19] that this phenomenon indicates a noncompetitive component of inhibition under the idea that

the enhancement of the inhibition was caused by a mechanism different from competitive one occurred by NDNBs in combination with high concentration of ACh. However, such a shift in the values of IC_{50} can also be explained by a change in the relationship between the receptor occupancy and the fraction of activated AChRs. As demonstrated in the upper panel of Fig. 4, the receptor occupancy O_{total} at which $[\mathrm{ARA}]_{\mathrm{peak}}/[\mathrm{ARA}]_{\mathrm{max}}$ (which corresponds to the relative current) takes the value of 0.5 increases with the decrease in the concentration of ACh, meaning that the IC_{50} increases with the decrease in the concentration of ACh. This shift in the IC_{50} is consistent with the observation in [9, 10] and occurs under a totally competitive mechanism of inhibition by an NDNB.

Interestingly, it was found that the relationship between the fraction of activated AChRs and the receptor occupancy became linear when the concentration of ACh was sufficiently large and the dissociation rate constants of an NDNB were sufficiently small. This finding may provide a reasonable justification of the use of the two-site model (2) in the analysis of kinetic constants for NDNBs through *in vitro* experiments. At least, the condition of large concentration of ACh is satisfied in the experiments reported in [4–8], where concentrations that opens about 93 % to 95 % of the AChRs were used. However, further consideration is needed to identify the conditions needed for the justification of the model (2), because the present study did not take into account the effect of desensitization of AChRs, which is the main cause of the decay in a measured current observed during *in vitro* experiments.

Conclusion

The relationship between the inhibition and the receptor occupancy by an NDNB was theoretically and numerically investigated. While a receptor binding model, which assumes a linear relationship, may be effective for estimating affinity of an NDNB through *in vitro* experiments, the model do not directly describe *in vivo* pharmacologic properties of NDNBs, because the nonlinearity between the inhibition and the receptor occupancy causes the modulation of the resultant concentration-effect relationships of NDNBs. It was found that the effect of characteristics of an NDNB on the extent of nonlinearity can be identified by a single parameter representing the site-selectivity of an NDNB.

Appendix

This appendix provides a dimensionless form of the model (3). As explained in the Methods section, nondimensionalization of the model can be conducted by introducing the dimensionless variables such as

$$\tau := t \cdot k_{\mathrm{hydrolysis}}, \quad x_{\mathrm{A}} := \frac{[\mathrm{A}]}{K_{\mathrm{A1}}}, \quad x_{\mathrm{ARA}} := \frac{[\mathrm{ARA}]}{[\mathrm{R}]_{\mathrm{total}}}, \quad x_{\mathrm{DRD}} := \frac{[\mathrm{DRD}]}{[\mathrm{R}]_{\mathrm{total}}}, \tag{18}$$

where $k_{\mathrm{hydrolysis}}$ stands for the rate constant of hydrolysis of ACh by acetylcholinesterase, K_{A1} for the dissociation equilibrium constant for ACh given by $k_{\mathrm{dissA1}}/k_{\mathrm{assocA1}}$, and $[\mathrm{R}]_{\mathrm{total}}$ for the concentration of the post-junctaional AChRs in the synaptic cleft. Similarly, the dimensionless variables x_{ARD}, x_{DRA}, x_{ARO}, x_{ORA}, x_{DRO}, and x_{ORD} for the remaining six complexes can be defined by dividing by

$[\mathrm{R}]_{\mathrm{total}}$. By substituting these dimensionless variables to the model (3), the following equations can be derived:

$$\begin{aligned}\frac{\mathrm{d}}{\mathrm{d}\tau}x_{\mathrm{A}} &= -x_{\mathrm{A}} + \kappa_{\mathrm{A1}}\lambda_{\mathrm{A1}}\{x_{\mathrm{ARA}} + x_{\mathrm{ARD}} + x_{\mathrm{ARO}} \\ &\quad - x_{\mathrm{A}}(x_{\mathrm{ORA}} + x_{\mathrm{ORD}} + x_{\mathrm{ORO}})\} \\ &\quad + \kappa_{\mathrm{A2}}\{\lambda_{\mathrm{A1}}(x_{\mathrm{ARA}} + x_{\mathrm{DRA}} + x_{\mathrm{ORA}}) \\ &\quad - \lambda_{\mathrm{A2}}x_{\mathrm{A}}(x_{\mathrm{ARO}} + x_{\mathrm{DRO}} + x_{\mathrm{ORO}})\}, \qquad (19\mathrm{a})\end{aligned}$$

$$\frac{\mathrm{d}}{\mathrm{d}\tau}x_{\mathrm{ARA}} = \kappa_{\mathrm{A1}}\left(x_{\mathrm{ORA}}x_{\mathrm{A}} - x_{\mathrm{ARA}}\right) + \kappa_{\mathrm{A2}}\left(\mu_{\mathrm{A}}x_{\mathrm{ARO}}x_{\mathrm{A}} - x_{\mathrm{ARA}}\right), \qquad (19\mathrm{b})$$

$$\frac{\mathrm{d}}{\mathrm{d}\tau}x_{\mathrm{DRD}} = \kappa_{\mathrm{D1}}\left(x_{\mathrm{ORD}}\delta - x_{\mathrm{DRD}}\right) + \kappa_{\mathrm{D2}}\left(\mu_{\mathrm{D}}x_{\mathrm{ORD}}\delta - x_{\mathrm{DRD}}\right), \qquad (19\mathrm{c})$$

$$\frac{\mathrm{d}}{\mathrm{d}\tau}x_{\mathrm{ARD}} = \kappa_{\mathrm{A1}}\left(x_{\mathrm{ORD}}x_{\mathrm{A}} - x_{\mathrm{ARD}}\right) + \kappa_{\mathrm{D2}}\left(\mu_{\mathrm{D}}x_{\mathrm{ARO}}\delta - x_{\mathrm{ARD}}\right), \qquad (19\mathrm{d})$$

$$\frac{\mathrm{d}}{\mathrm{d}\tau}x_{\mathrm{DRA}} = \kappa_{\mathrm{D1}}\left(x_{\mathrm{ORA}}\delta - x_{\mathrm{DRA}}\right) + \kappa_{\mathrm{A2}}\left(\mu_{\mathrm{A}}x_{\mathrm{DRO}}x_{\mathrm{A}} - x_{\mathrm{DRA}}\right), \qquad (19\mathrm{e})$$

$$\begin{aligned}\frac{\mathrm{d}}{\mathrm{d}\tau}x_{\mathrm{ARO}} &= \kappa_{\mathrm{A1}}\left(x_{\mathrm{ORO}}x_{\mathrm{A}} - x_{\mathrm{ARO}}\right) + \kappa_{\mathrm{A2}}\left(x_{\mathrm{ARA}} - \mu_{\mathrm{A}}x_{\mathrm{ARO}}x_{\mathrm{A}}\right) \\ &\quad + \kappa_{\mathrm{D2}}\left(x_{\mathrm{ARD}} - \mu_{\mathrm{D}}x_{\mathrm{ARO}}\delta\right), \qquad (19\mathrm{f})\end{aligned}$$

$$\begin{aligned}\frac{\mathrm{d}}{\mathrm{d}\tau}x_{\mathrm{ORA}} &= \kappa_{\mathrm{A2}}\left(\mu_{\mathrm{A}}x_{\mathrm{ORO}}x_{\mathrm{A}} - x_{\mathrm{ORA}}\right) + \kappa_{\mathrm{A1}}\left(x_{\mathrm{ARA}} - x_{\mathrm{ORA}}x_{\mathrm{A}}\right) \\ &\quad + \kappa_{\mathrm{D1}}\left(x_{\mathrm{DRA}} - x_{\mathrm{ORA}}\delta\right), \qquad (19\mathrm{g})\end{aligned}$$

$$\begin{aligned}\frac{\mathrm{d}}{\mathrm{d}\tau}x_{\mathrm{DRO}} &= \kappa_{\mathrm{D1}}\left(x_{\mathrm{ORO}}\delta - x_{\mathrm{DRO}}\right) + \kappa_{\mathrm{A2}}\left(x_{\mathrm{DRA}} - \mu_{\mathrm{A}}x_{\mathrm{DRO}}x_{\mathrm{A}}\right) \\ &\quad + \kappa_{\mathrm{D2}}\left(x_{\mathrm{DRD}} - \mu_{\mathrm{D}}x_{\mathrm{DRO}}\delta\right), \qquad (19\mathrm{h})\end{aligned}$$

$$\begin{aligned}\frac{\mathrm{d}}{\mathrm{d}\tau}x_{\mathrm{ORD}} &= \kappa_{\mathrm{D2}}\left(\mu_{\mathrm{D}}x_{\mathrm{ORO}}\delta - x_{\mathrm{ORD}}\right) + \kappa_{\mathrm{A1}}\left(x_{\mathrm{ARD}} - x_{\mathrm{ORD}}x_{\mathrm{A}}\right) \\ &\quad + \kappa_{\mathrm{D1}}\left(x_{\mathrm{DRD}} - x_{\mathrm{ORD}}\delta\right). \qquad (19\mathrm{i})\end{aligned}$$

Funding

This work was supported in part by Grant-in-Aid for Scientific Research (KAKENHI) from the Japan Society for Promotion of Science (#20K04553).

Abbreviations

NDNB: Nondepolarizing neuromuscular blocking drugs, ACh: Acetylcholine, AChR: Acetylcholine receptor

Competing interests

The authors declare that they have no competing interests.

Author details

[1]Department of Electrical Materials and Engineering, University of Hyogo, Hyogo, Japan. [2]Department of Anesthesiology, Kagawa University, Kagawa, Japan.

References

1. Pardo, M.C., Miller, R.D.: Basics of Anesthesia, 7th edn. Elsevier, Philadelphia (2018)
2. Yost, C.S., Winegar, B.D.: Potency of agonists and competitive antagonists on adult- and fetal-type nicotinic acetylcholine receptors. Cellular and Molecular Neurobiology **17**(1), 35–50 (1997). doi:10.1023/A:1026325020191
3. Paul, M., Kindler, C.H., Fokt, R.M., Dresser, M.J., Dipp, N.C.J., Yost, C.S.: The potency of new muscle relaxants on recombinant muscle-type acetylcholine receptors. Anesthesia & Analgesia **94**(3), 597–603 (2002). doi:10.1097/00000539-200203000-00022
4. Wenningmann, I., Dilger, J.P.: The kinetics of inhibition of nicotinic acetylcholine receptors by (+)-tubocurarine and pancuronium. Molecular Pharmacology **60**(4), 790–796 (2001). https://molpharm.aspetjournals.org/content/60/4/790.full.pdf

5. Demazumder, D., Dilger, J.P.: The kinetics of competitive antagonism by cisatracurium of embryonic and adult nicotinic acetylcholine receptors. Molecular Pharmacology **60**(4), 797–807 (2001). https://molpharm.aspetjournals.org/content/60/4/797.full.pdf
6. Demazumder, D., Dilger, J.P.: The kinetics of competitive antagonism of nicotinic acetylcholine receptors at physiological temperature. The Journal of Physiology **586**(4), 951–963 (2008). doi:10.1113/jphysiol.2007.143289
7. Liu, M., Dilger, J.P.: Synergy between pairs of competitive antagonists at adult human muscle acetylcholine receptors. Anesthesia & Analgesia **107**(2), 525–533 (2008). doi:10.1213/ane.0b013e31817b4469
8. Liu, M., Dilger, J.P.: Site selectivity of competitive antagonists for the mouse adult muscle nicotinic acetylcholine receptor. Molecular Pharmacology **75**(1), 166–173 (2009). doi:10.1124/mol.108.051060
9. Jonsson, M., Gurley, D., Dabrowski, M., Larsson, O., Johnson, E.C., Eriksson, L.I.: Distinct Pharmacologic Properties of Neuromuscular Blocking Agents on Human Neuronal Nicotinic Acetylcholine Receptors: A Possible Explanation for the Train-of-four Fade. Anesthesiology **105**(3), 521–533 (2006). doi:10.1097/00000542-200609000-00016
10. Fagerlund, M.J., Dabrowski, M., Eriksson, L.I.: Pharmacological characteristics of the inhibition of nondepolarizing neuromuscular blocking agents at human adult muscle nicotinic acetylcholine receptor. Anesthesiology **110**, 1244–1252 (2009). doi:10.1097/ALN.0b013e31819fade3
11. Dilger, J.P., Steinbach, J.H.: Inhibition of muscle acetylcholine receptors by nondepolarizing drugs: Humans are not unique. Anesthesiology **112**, 247–249 (2010). doi:10.1097/ALN.0b013e3181c5dbbc
12. Gabrielsson, J., Weiner, D.: Pharmacokinetic and Pharmacodynamic Data Analysis: Concepts and Applications, 5th edn. Swedish Pharmaceutical Press, Stockholm (2016)
13. Nigrovic, V., Amann, A.: Competition between acetylcholine and a nondepolarizing muscle relaxant for binding to the postsynaptic receptors at the motor end plate: Simulation of twitch strength and neuromuscular block. Journal of Pharmacokinetics and Pharmacodynamics **30**(1), 23–51 (2003). doi:10.1023/A:1023245409315
14. Akk, G., Auerbach, A.: Inorganic, monovalent cations compete with agonists for the transmitter binding site of nicotinic acetylcholine receptors. Biophysical Journal **70**(6), 2652–2658 (1996). doi:10.1016/S0006-3495(96)79834-X
15. Langtangen, H.P., Pedersen, G.K.: Scaling of Differential Equations. Springer, Cham (2016)
16. Kokotović, P., Khalil, H., O'Reilly, J.: Singular Perturbation Methods in Control: Analysis and Design. Society for Industrial and Applied Mathematics, Philadelphia (1999). doi:10.1137/1.9781611971118
17. Kuehn, C.: Multiple Time Scale Dynamics. Springer, Cham (2015)
18. Paton, W.D.M., Waud, D.R.: The margin of safety of neuromuscular transmission. The Journal of Physiology **191**(1), 59–90 (1967). doi:10.1113/jphysiol.1967.sp008237. https://physoc.onlinelibrary.wiley.com/doi/pdf/10.1113/jphysiol.1967.sp008237
19. Fagerlund, M.J., Eriksson, L.I.: Current concepts in neuromuscular transmission. British Journal of Anaesthesia **103**(1), 108–114 (2009). doi:10.1093/bja/aep150. http://oup.prod.sis.lan/bja/article-pdf/103/1/108/17424609/aep150.pdf

Figures

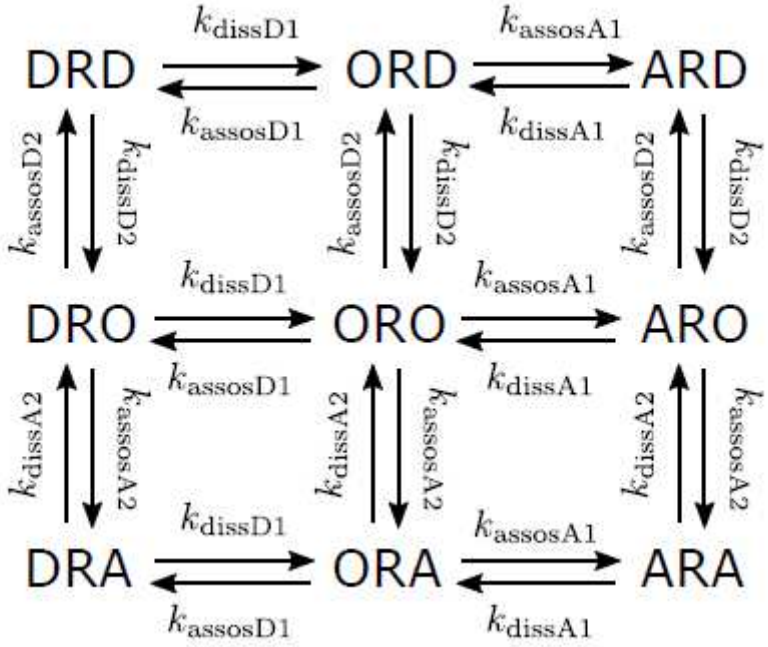

Figure 1

Diagram of the interactions between acetylcholine (A), NDNB (D), and the postsynaptic receptor (R). The complexes formed by binding of ACh and NDNB to AChR are represented by 3-letter symbols, where the rst and last letters denote the rst and second ligands occupying the sites 1 and 2, respectively. The complex ARA represents the activated AChR.

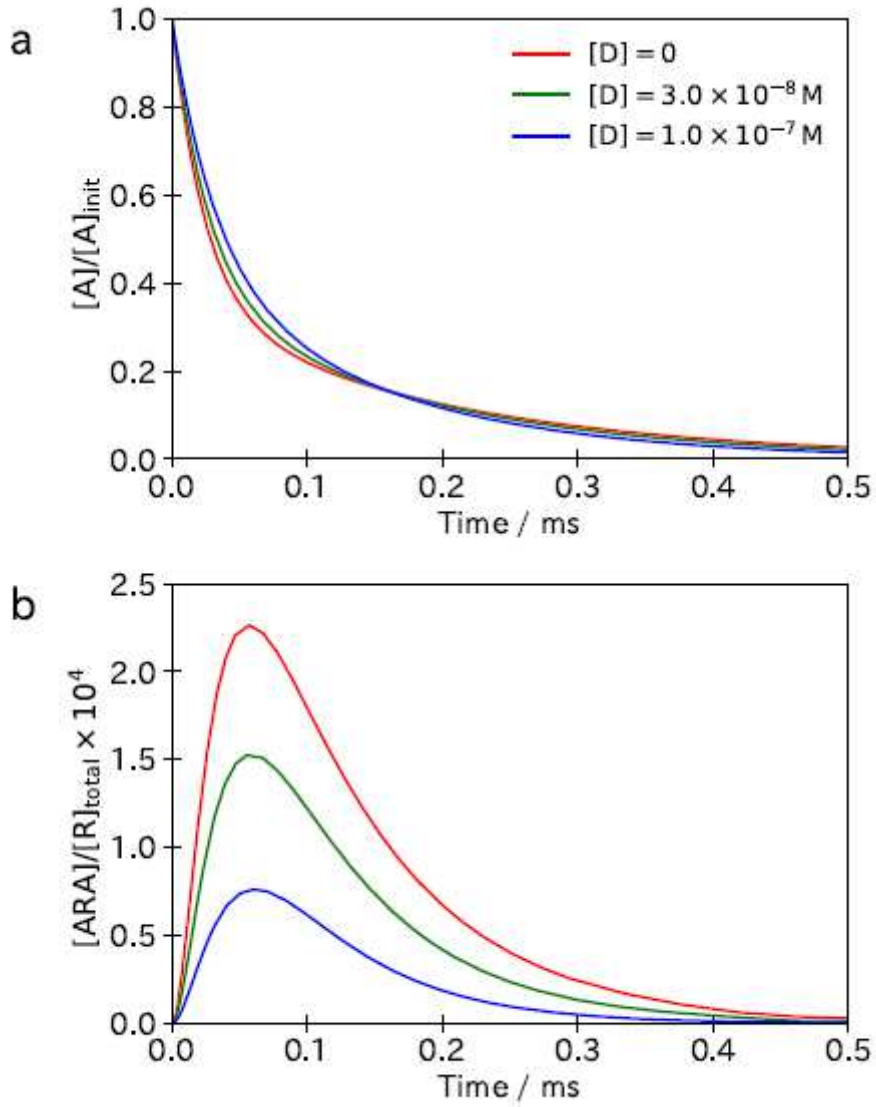

Figure 2

An example of simulation results of the model (3). a The time course of the concentration [A] of free ACh. b The time course of the concentration [ARA] of the complex ARA representing the activated AChRs.

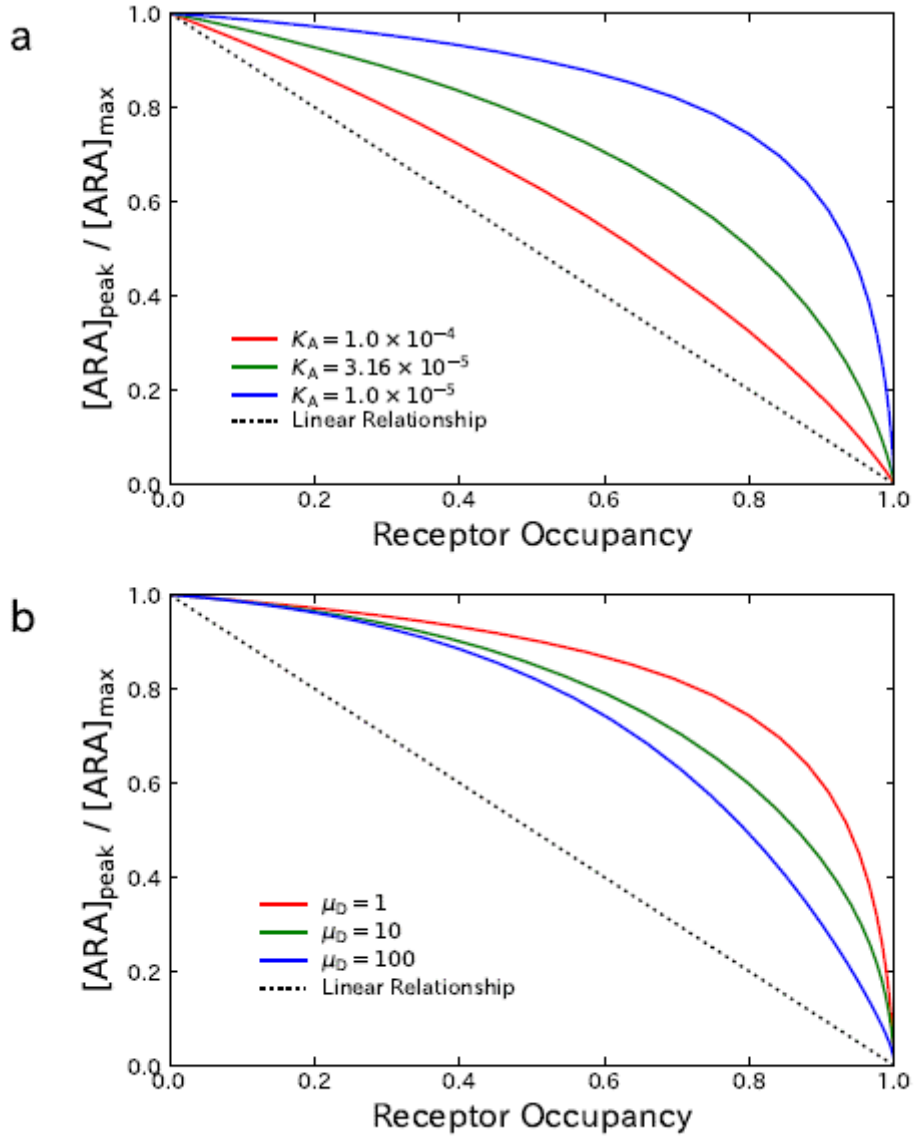

Figure 3

Effect of varying kinetic constants for ACh and NDNB on the relationship between the fraction of activated AChRs, [ARA]peak=[ARA]max, and the receptor occupancy Ototal. a Results of varying the equilibrium dissociation constants for ACh under KA = KA1 = KA2 (kA1 = kA2 and μA = 1). b Results of varying the site-selectivity μD = KD1=KD2 of an NDNB.

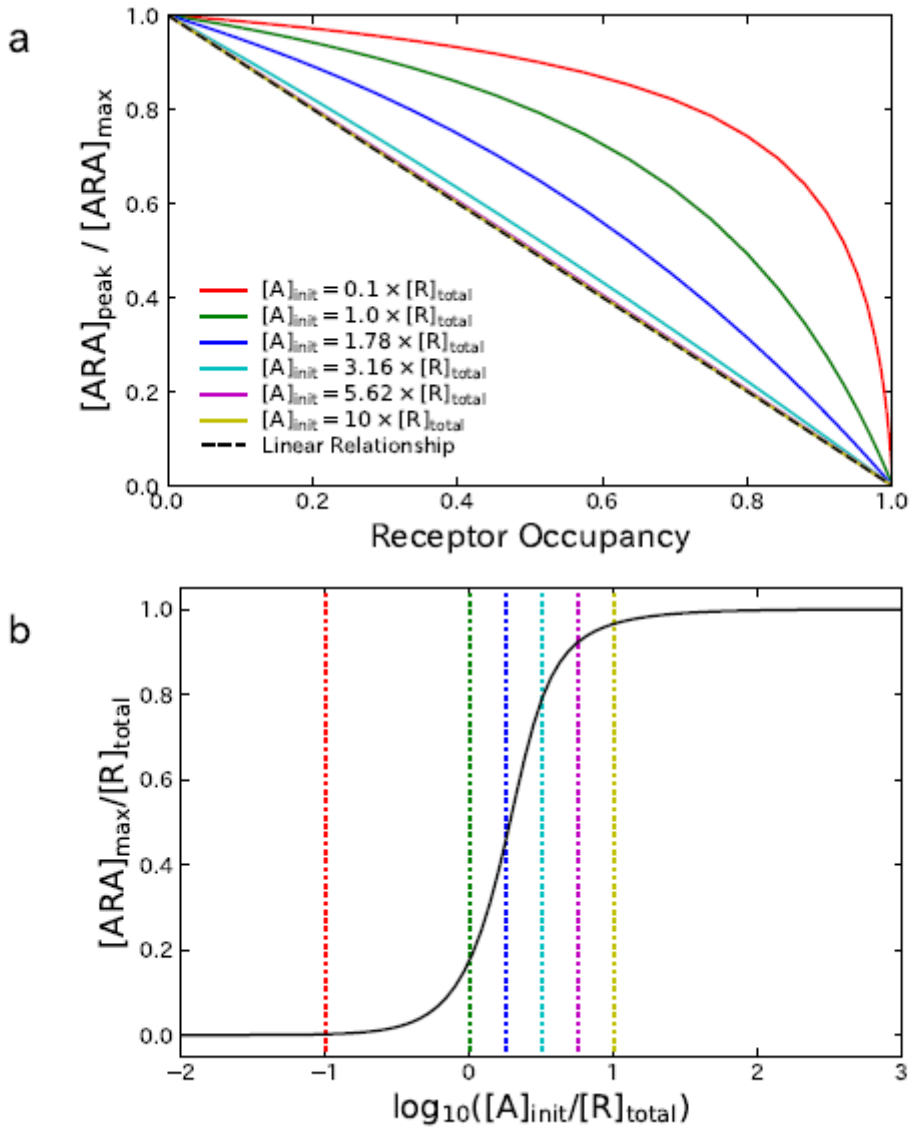

Figure 4

Effect of varying the initial concentration [A]init of ACh on the numerical results. a The relationship between the fraction of activated AChRs, [ARA]peak=[ARA]max, and the receptor occupancy Ototal under various settings of [A]init. b The concentration-effect relationship between the activated AChRs in the absence of NDNBs and the initial concentration [A]init.

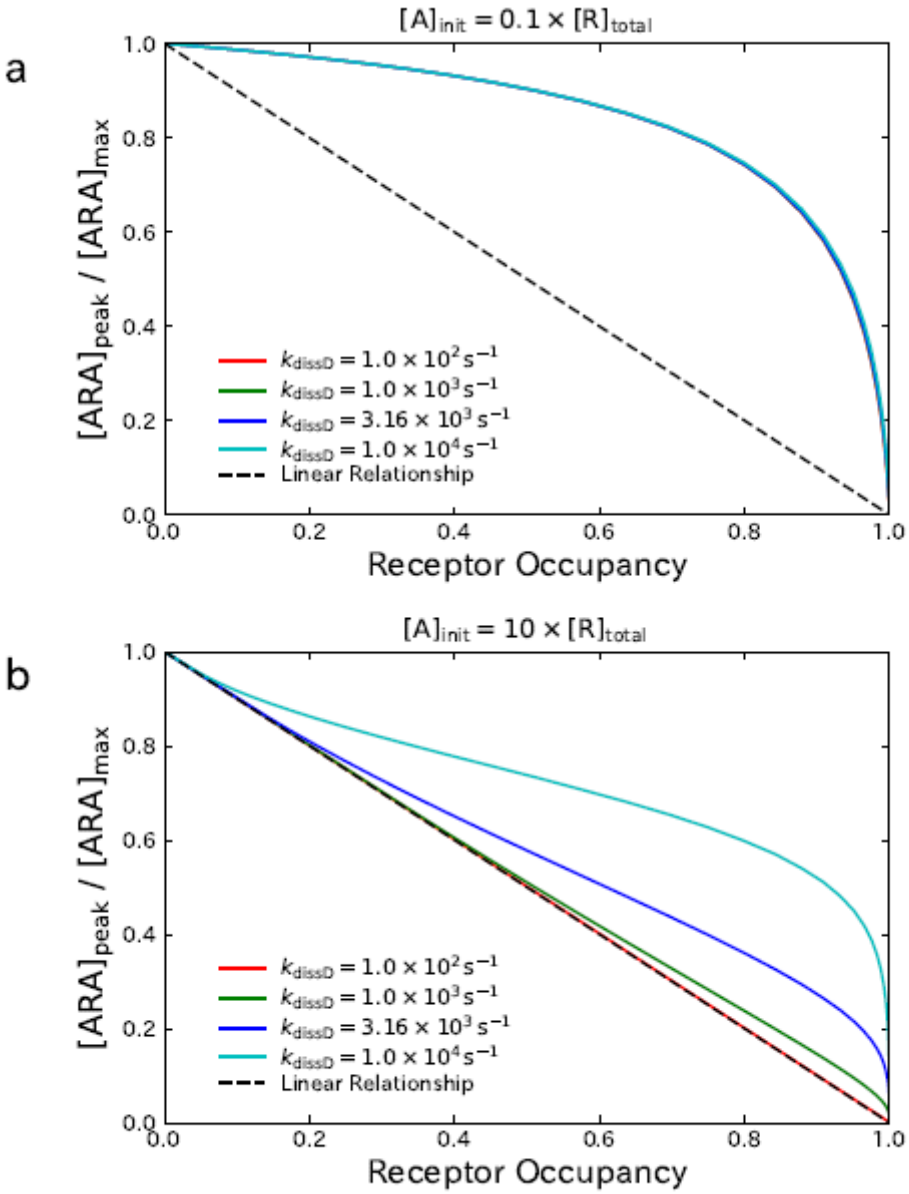

Figure 5

Effect of varying the dissociation rate constants kdissD1 and kkdissD2 on the relationship between the fraction of activated AChRs, [ARA]peak=[ARA]max, and the receptor occupancy Ototal. a Results under the setting of [A]init = 0:1 x [R]total corresponding to in vivo concentration. b Results under the setting of [A]init = 10 x [R]total corresponding to in vitro concentration.